EPJ Web of Conferences **362**, 01002 (2026) https://doi.org/10.1051/epjconf/202636201002
ILRC31/CLRC22-2024

Constraining aerosol properties with the camera lidar

John E. Barnes [(a)], **Nimmi C. P. Sharma** [(b)], **Amin S. Kabir**[(c)]
[(a)] *NOAA/Global Monitoring Lab, Retired, 127 S Hoover Ave, Louisville, Colorado, USA*
[(b)] *Dept. of Physics and Engineering Physics, Central Connecticut State University, New Britain, CT, USA*
(c) Department of Physical and Earth Sciences, University of The Bahamas, Nassau, The Bahamas
BarnesBJE@gmail.com

Abstract: An aerosol measurement campaign was carried out in the summer of 2022 at a NOAA (National Oceanic and Atmospheric Administration) field site north of Boulder, Colorado, USA. Two camera lidars were deployed at 532 and 808 nm. The unique properties of the camera lidar include aerosol profiles all the way to the ground at high resolution where they can be compared with in-situ measurements. Surface aerosol measurements included three-wavelength total scatter and absorption, as well as condensation nuclei and particle size distributions. The camera lidar extinctions at the surface compared well with the in-situ extinctions. The 532/808 Angstrom exponent in the Planetary Boundary Layer was 1.0 and for an upper tropospheric layer it was 2.5 indicating smaller particles.

1. Introduction

Characterizing aerosols is complicated due to the wide variety of compositions, size distributions, shapes, sources, and removal processes. A further complication is that these vary with altitude. Ground-based lidar complements in-situ sampling by aircraft, balloons, and drones by offering continuous sampling at a single location but for extended periods of time. Satellite instruments offer global coverage but at a reduced sampling interval and, with some instruments, a much reduced spatial resolution.

This paper describes measurements made by a camera lidar [1-4]. Although limited to twilight and nighttime conditions the technique has interesting advantages when compared to lidar. Taking advantage of the high altitude resolution at the surface and no overlap function, the camera lidar can be compared to in-situ measurements. A campaign was organized in 2022 to demonstrate these capabilities.

2. Campaign Location

The National Oceanic and Atmospheric Administration (NOAA) operates a test facility on a mesa north of Boulder, Colorado (Lat: 40.13, Long: 105.24 W, Alt 1691 m). The site is rural and is near the foothills of the Rocky Mountains. Atmospheric transport can be directly from the mountains or can come from the urban areas of Boulder, Denver, and other smaller cities. The conditions during the campaign (2022/5/29-2022/6/4) were low aerosol loading indicating mountain air.

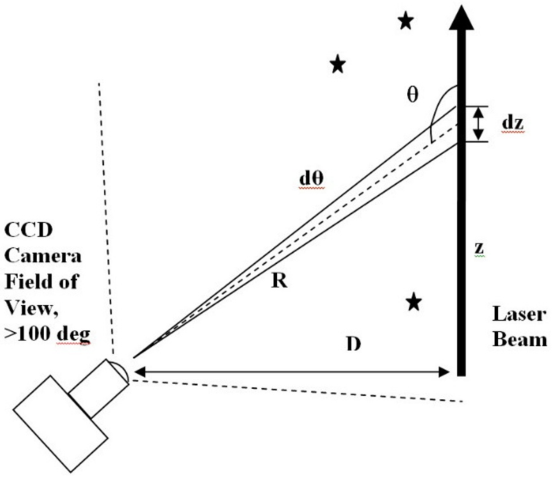

Figure 1. Components of the camera lidar. Stars in the image can be used to calculate AOD.

3. Camera Lidar

The camera lidar (CLidar) uses a CCD camera with a wide-angle (Fisheye) lens to image a vertically pointed laser from the ground to the zenith [1,2]. No scanning is required. An interference filter is inserted between the lens and camera to reduce background light. An inexpensive continuous wave (CW) laser can be used, or the camera can be used with a conventional pulsed-laser lidar to get high resolution data in the boundary layer. The range measurement is due strictly to the geometry and no electronics are needed besides what is contained in the camera. Fig. 1 and Table 1 describe the geometry and equipment. The camera and laser were separated by 108.7 m at the surface for this campaign. The 808 nm laser was chosen because it is relatively inexpensive for the power, gives good separation from the 532 nm, and still has good sensitivity for the camera.

The camera is cooled to reduce dark noise and a simple shutter controls the exposure time which is usually a few minutes. The system is fairly portable and can be run on batteries if needed. An important quality of the lens is that it images an equal solid angle onto each pixel. This means the altitude resolution decreases as altitude increases. Near the ground the resolution is about 0.06 meters and has decreased to 80 meters at 4 km altitude. The stratosphere is measured coarsely but is still useful for normalization.

Table 1. Camera Lidar Components

Component		Value
Green CW laser		3 Watt
λ	Wavelength	532 nm
Infrared CW laser		5 Watt
λ	Wavelength	808 nm
Camera SBIG,	STF-8300M	6 M Pix
Chip size	17.96 -13.52	mm
Interference Filters	FWHH	10 nm
Lens - Sigma	FL 10 mm	F/2.8
Camera/Laser	Separation	108.7 m

4. Aerosol Phase Functions

The standard aerosol lidar technique measures 180 degree backscattered light ($m^{-1}sr^{-1}$). Converting to a more useful quantity like aerosol extinction (m^{-1}) requires an assumption of the extinction to backscatter ratio (sr) which varies widely. For example the ratio varies from 20 to 70 for the six aerosol types used by the NASA space lidar CALIPSO [5,6].

The camera lidar measures scattered light starting at 90 degrees and quickly approaches 180 and more of the aerosol phase function (APF) must be assumed. In figure 2, two of the CALIPSO APFs are shown along with an APF retrieved from AERONET [7,8] data taken near the campaign site. None of the APFs have been directly measured. For this campaign a variety of APFs were tested to find the best match to the data.

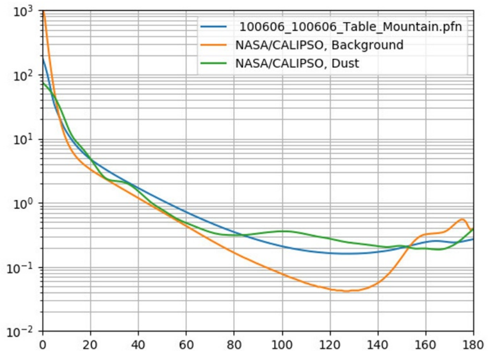

Figure 2. Aerosol Phase Functions calculated (NASA/CALIPSO) or retrieved AERONET. The value at 180 degrees determines the lidar extinction to backscatter ratio.

5. Normalization

To normalize a lidar signal it is assumed that the ratio of aerosol to molecular scatter is known at a given altitude. Usually it is assumed to be a high altitude free of aerosol. The CLidar technique is quite similar but has a distinctly different shape of the molecular density curve [1,2].

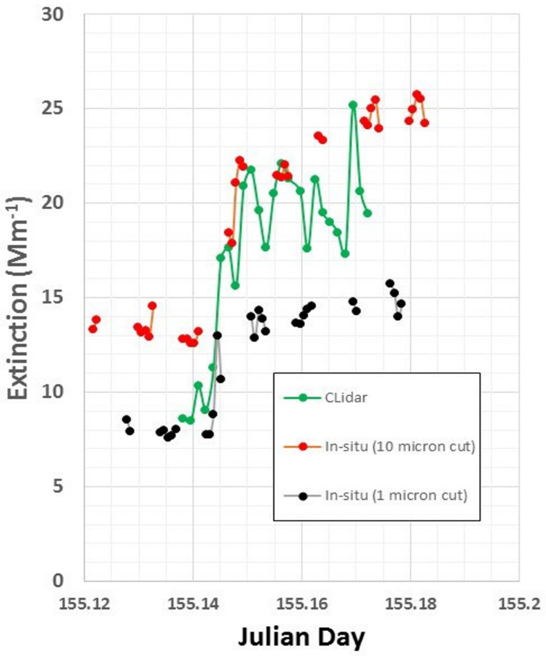

Figure 3. Surface aerosol system (10 m intake) compared to CLidar profile (2022/6/4).

Clouds and high altitude aerosol layers can interfere with the normalization. The camera lidar can use an additional constraint by comparing the profile at the surface with in-situ instruments. In figure 3 the surface extinction (total scatter + absorption) is compared for the camera lidar (CLidar) and the in-situ. The in-situ sampling system alternates between a one micron and a 10 micron impactor. The impactors remove particles larger than one or 10 microns respectively. The CLidar wavelength of 532 nm is compared to the in-situ Total Scatter (550 nm) plus absorption (528 nm). No adjustments for wavelength have been made.

It was found that the AERONET retrieved APF provided the best match of extinction at the surface. This is essentially constraining the value of the APF at 90 degrees.

6. Stellar Aerosol Optical Depth

Stars in the camera images can be used to measure aerosol optical depth (AOD) [9,10]. Having the AOD at the same wavelength, location, and time as the profile, with no additional equipment, is an extremely useful constraint on the integrated CLidar profile. For a sun photometer, the instrument must be calibrated either at a very clean location or against a standard instrument. The calibration quantifies two constants, the slope of the photometer response and extraterrestrial signal.

The star photometer can also be calibrated this way, but it can also use pairs of stars and their measured magnitudes avoiding the calibration. Care must be taken to avoid biases due to double and variable stars, and differences in color indices. In this paper the web program Stellarium [11] has been used to identify stars in the camera images, and to provide the magnitude, air mass, and color index. The signal from a star in a camera image is calculated with a pixel summing algorithm.

7. Results

Five nights of measurements were made during the campaign. A representative profile from the first night (2022/5/29) is shown in figure 4 for both wavelengths. That night there was a broad aerosol layer in the upper troposphere.

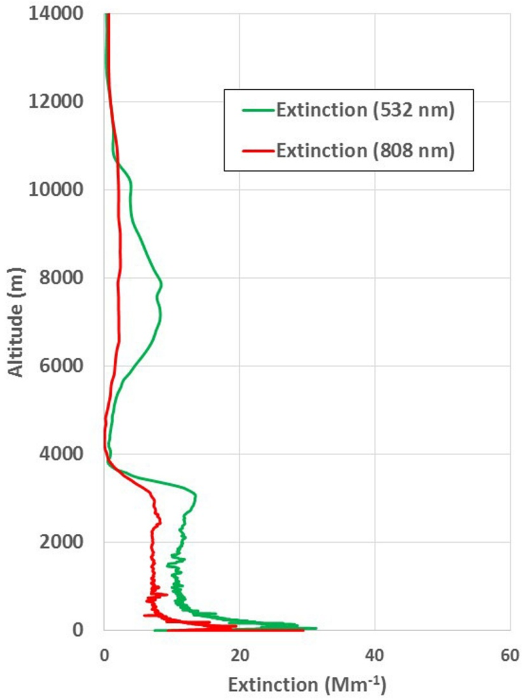

Figure 4. Extinction profiles at the two laser wavelengths, 532 and 808 nm.

In figure 5 the same data are shown for the first 1000 m. The very high altitude resolution is seen and a peak at 100 m is easily resolved which would be difficult with a lidar. The signal is determined by fitting a Gaussian plus constant function to a cross-section of the beam in the camera image pixel by pixel. The constant quantifies the background. The spikes in the profiles are usually places where the fit was effected by stars near the beam.

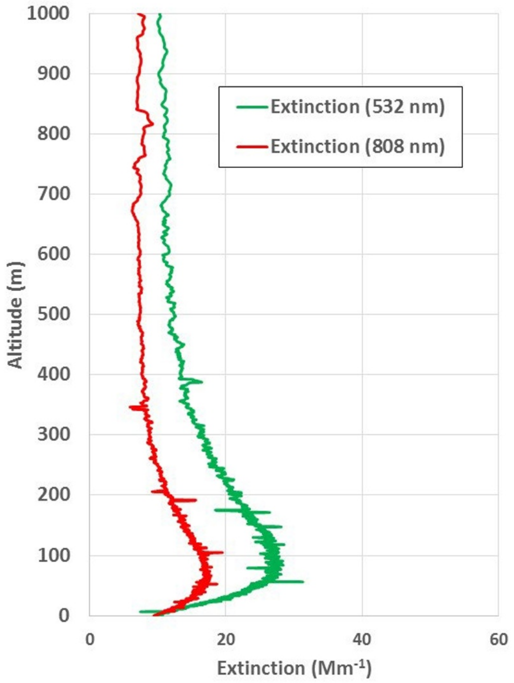

Figure 5. Extinction profiles at the two laser wavelengths, 532 and 808 nm.

With lidars, two wavelengths can be used to calculate a color exponent. With the camera lidar the profiles have already been converted to extinctions, so an Angstrom exponent can be calculated. For the profiles shown the average Angstrom exponents were calculated for the intervals 0 to 300 m, 500 to 2000 m, and 6000 to 11000 m. The exponents were 1.01, 1.01, and 2.53 respectively indicating smaller particles in the upper tropospheric layer. This also indicates the peak at 100 m has the same intrinsic aerosol properties as the rest of the boundary layer.

The AOD for the integrated profile in figure 4 is 0.107. Sun photometer measurements were available the day before and after the profile was taken. The AODs were 0.1015 +/- 0.0045 and 0.1071 +/- 0.0047 indicating the aerosol loading may have been fairly constant during the night. The stellar AOD was measured with two pairs of stars, Alkaid-Caph and Alioth-Caph for 5 files (10 minutes). The 10 measurements averaged 0.114 +/- 0.0152. The agreement of the AOD of the camera lidar profile with the sun and stellar AODs lends confidence that the chosen aerosol phase function is a good representation that night's aerosol properties.

8. Further Work

The very low peak seen in figure 5 has been seen in other locations with the camera lidar. Explanations in boundary layer meteorology are being pursued.

9. References

[1] Barnes, J. E., S. Bronner, R. Beck, and N. C. Parikh: Boundary layer scattering measurements with a CCD camera lidar, Applied Optics, 42, 2647-2652 (2003).

[2] Barnes, John E., N. C. Parikh Sharma and Trevor B. Kaplan, Atmospheric aerosol profiling with a bistatic imaging lidar system, Applied Optics, 46, 2922-2929 (2007).

[3] Sharma, N. C. Parikh; Barnes, John E.; Kaplan, Trevor B.; Clarke, Antony D., Coastal aerosol profiling with a camera lidar and nephelometer, J. of Atmos. Oceanic Technology, 28, 418-425 (2011).

[4] Yuxuan Bian, et. al, A novel method to retrieve the nocturnal boundary layer structure based on CCD laser aerosol detection system measurements, Remote Sensing Environ. 211, doi.org/10.1016/j.rse.2018.04.007 (2018)

[5] CALIPSO team, aerosol phase functions, personal communication.

[6] Omar., A. H., et al., The CALIPSO automated aerosol classification and lidar ratio selection algorithm, J. of Atmos. Oceanic Technology, 26, 1994-2014 (2009).

[7] http://aeronet.gsfc.nasa.gov/

[8] Holben, B. N., et al.: AERONET—A federated instrument network and data archive for aerosol characterization, Remote Sens. Environ., 66, 1–16 (1998).

[9] C Leiterer, U., et al.: A new star photometer developed for spectral aerosol optical thickness measurements in Lindenberg, Beitr. Phys. Atmosph., 68, 133-141 (1995).

[10] Perez-Ramirez, D. et al., Development and calibration of a star photometer to measure the aerosol optical depth: smoke observations at a high mountain site, Atmos. Environ., 42, 2733-2738 (2008).

[11] https://stellarium.org/